RESEARCH ARTICLE

Bacterivory by phototrophic picoplankton and nanoplankton in Arctic waters

Robert W. Sanders[1] & Rebecca J. Gast[2]

[1]Department of Biology, Temple University, Philadelphia, PA, USA; and [2]Biology Department, Woods Hole Oceanographic Institution, Woods Hole, MA, USA

Correspondence: Robert W. Sanders, Biology Life Sciences, Temple University, 1900 North 12th Street, Philadelphia, PA 19122, USA. Tel.: +1 1215 204 2056; fax: +1 1215 204 6646; e-mail: robert.sanders@temple.edu

Received 24 July 2011; revised 26 October 2011; accepted 6 November 2011.
Final version published online 5 December 2011.

DOI: 10.1111/j.1574-6941.2011.01253.x

Editor: Patricia Sobecky

Keywords
Arctic Ocean; DGGE; mixotrophy; phytoflagellates; picoeukaryotes.

Abstract

Mixotrophy, the combination of phototrophy and heterotrophy within the same individual, is widespread in oceanic systems. Yet, neither the presence nor ecological impact of mixotrophs has been identified in an Arctic marine environment. We quantified nano- and picoplankton during early autumn in the Beaufort Sea and Canada Basin and determined relative rates of bacterivory by heterotrophs and mixotrophs. Results confirmed previous reports of low microbial biomass for Arctic communities in autumn. The impact of bacterivory was relatively low, ranging from 0.6×10^3 to 42.8×10^3 bacteria mL^{-1} day^{-1}, but it was often dominated by pico- or nanomixotrophs. From 1% to 7% of the photosynthetic picoeukaryotes were bacterivorous, while mixotrophic nanoplankton abundance comprised 1–22% of the heterotrophic and 2–32% of the phototrophic nanoplankton abundance, respectively. The estimated daily grazing impact was usually < 5% of the bacterial standing stock, but impacts as high as 25% occurred. Analysis of denaturing gradient gel electrophoresis (DGGE) band patterns indicated that communities from different depths at the same site were appreciably different and that there was a shift in community diversity at the midpoint of the cruise. Sequence information from DGGE bands reflected microbes related to those from other Arctic studies, particularly from the Beaufort Sea.

Introduction

Planktonic protists have traditionally been categorized based on their modes of energy and carbon acquisition as either phototrophic (algal) or heterotrophic. However, mixotrophic behavior, whereby organisms combine both of these nutritional modes within a single cell, has been increasingly recognized and documented in aquatic systems (Stoecker *et al.*, 2009; Sanders, 2011). Phagotrophic feeding behavior occurs in a variety of algal taxa, including chrysophytes, dinoflagellates, prymnesiophytes, rhaphidophytes and cryptophytes, and these organisms have been shown to be ecologically significant as primary producers and consumers (Sanders & Porter, 1988; Unrein *et al.*, 2007; Jeong *et al.*, 2010; Jeong, 2011). Mixotrophic nanoplankton (MNAN) can comprise up to 50% of the total phototrophic nanoplankton (PNAN) (cells < 20 μm) and be responsible for as much as 86% of the total bacterivory in diverse aquatic habitats (e.g. Sanders *et al.*, 1989; Havskum & Riemann, 1996; Havskum & Hansen, 1997; Sanders *et al.*, 2000).

Although abundances and bacterivory by protists have been examined in the Arctic Ocean, there are no previous investigations of mixotrophy. Earlier studies in the central Arctic Ocean and Chukchi Sea found heterotrophic nanoplankton (HNAN) comprised a large portion of the microbial biomass during summer when flagellates in the 6 to 20-μm-size range tended to dominate HNAN biomass (Sherr *et al.*, 1997); autotrophic plankton biomass during that investigation was dominated by dinoflagellates and miscellaneous flagellates at most stations in the central Arctic, with diatoms making up most of the remaining biomass (Booth & Horner, 1997). However, at some stations in the Canada and Makarov Basins, particularly under thicker ice cover, picophytoflagellates (cells < 2.5 μm) tentatively identified as *Micromonas* sp. contributed up to

FEMS MICROBIOLOGY ECOLOGY

93% of autotrophic cell abundance and 36% of the autotrophic biomass in freshly prepared samples (Booth & Horner, 1997; Sherr *et al.*, 1997).

In the present study, the occurrence of mixotrophy in pico- and nanophytoplankton from Arctic waters was assessed, abundances and bacterivory of heterotrophic and phototrophic protists were determined, and a molecular analysis of the potentially abundant protists was performed using denaturing gradient gel electrophoresis (DGGE). We hypothesized that mixotrophy could be a successful strategy for these Arctic phototrophs based upon the ubiquitous incidence of MNAN in subpolar and Antarctic waters (Nygaard & Tobiesen, 1993; Havskum & Riemann, 1996; Bell & Laybourn-Parry, 2003; Moorthi *et al.*, 2009). We expected that the grazing impacts of mixotrophic organisms could sometimes exceed that of the heterotrophic plankton in the Beaufort Sea and the Canada Basin region of the Arctic Ocean.

Materials and methods

Study sites and sampling

Samples to examine protistan abundance and bacterivory were collected at 10 stations within the Beaufort Sea and the Canada Basin of the Arctic Ocean on a cruise of opportunity aboard the icebreaker USCGC Healy in September 2008 (Fig. 1). Water was collected from the deep chlorophyll maximum layer (DCM) and at 5 m below the surface during the upcast of a rosette CTD system with 10-L Niskin bottles. These depths were considered to be representative of the mixed surface layer or of a depth (DCM) with potentially increased biomass and activity of microorganisms, including phytoplankton. Exact station locations and physical parameters of the sampling depths from the CTD instruments are presented in Table 1.

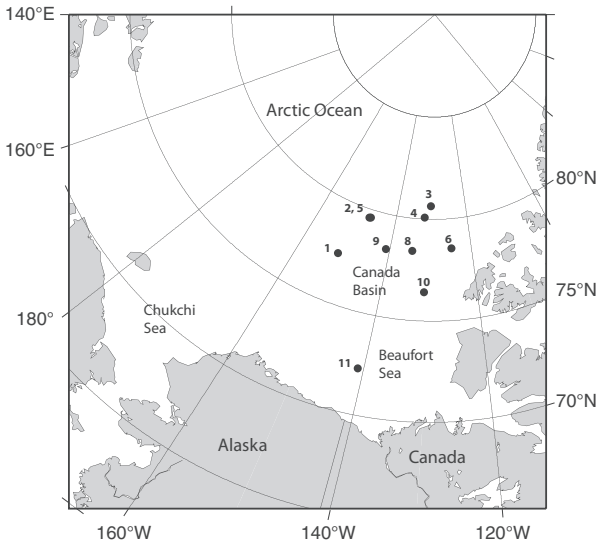

Fig. 1. Location of sampling sites within the Beaufort Sea and Canada Basin. North Pole is at the upper edge of the chart.

Subsamples from each depth were collected immediately for microplankton counts and chlorophyll *a* analysis. Microplankton (ciliates, dinoflagellates, other microflagellates, and diatoms) were preserved with Lugol's solution (4.5% final concentration) and later settled and enumerated using an inverted microscope at a magnification of 200×. For each chlorophyll *a* determination, 100 mL of whole water was filtered onto a 47-mm GF/F filter (Whatman) and frozen at −20 °C until analyzed. Filters were later extracted in 90% acetone overnight at −20 °C, and fluorescence was determined with a Model TD-700 fluorometer (Turner Designs, Sunnyvale, CA).

Preparation of fluorescently labeled bacteria (FLB)

FLB were prepared from cultured *Halomonas halodurans* (*c.* 1 μm). These were used successfully in prior studies for the identification of MNAN (Sanders *et al.*, 2000; Moorthi *et al.*, 2009). *Halomonas halodurans* was inoculated into 1 L of 0.2-μm-filtered and autoclaved seawater enriched with yeast extract (0.1% final concentration). Bacterial cells were grown at room temperature, harvested by centrifugation, washed using filter-sterile seawater (FSW), and then stained with mixing for 3 h at 64 °C with 5-(4,6-dichlorotriazin-2-yl) aminofluorescein (DTAF; Sigma-Aldrich Co., St. Louis, MO) at a concentration of 40 μg mL^{-1}. FLB were then washed 4–5 times with FSW by repeated centrifugation, and finally filtered through sterile 47-mm polycarbonate filters (Whatman, 3 μm pore size) to remove clumps. Concentrations of FLB were determined with epifluorescence microscopy, and aliquots of FLB were stored at −20 °C until just prior to use in experiments.

Experimental setup and processing

For feeding experiments, triplicate 2-L samples of seawater, prescreened through 100-μm Nitex mesh (Wildlife Supply, Yulee, FL) to remove zooplankton, were incubated in 2.7-L polycarbonate bottles. Zooplankton were not observed in the experimental bottles or on any of the slides when the samples were counted.

To determine the appropriate addition of tracer particles, bacterial abundance from each depth was initially assessed by epifluorescence microscopy from samples filtered on 25-mm black Poretics polycarbonate filters (0.2 μm pore size). Filters were stained and mounted with cover slips onto glass slides using VectaShield®

Table 1. Sampling stations, date (in 2008), locations (lat/long), collection depth (m), water column depth Z_{max} (m), salinity (PSU), temperature (°C), and light (quanta cm^{-2} s^{-1} × 10^{15})

Station	Date	Location	Depth	Z_{max}	Salinity	Temp	PAR
1	7 September	77°24.53′N	5	3840	27.43	−1.12	2.33
		151°18.84′W	60		31.01	−1.08	0.08
2	8 September	79°34.20′N	5	3820	28.14	−1.39	4.63
		147°13.75′W	50		31.30	−1.45	0.21
3	11/12 September	80°36.97′N	5	3500	28.97	−1.56	0.02
		130°21.72′W	50		30.79	−1.44	0.01
4	13 September	80°03.84′N	5	3620	27.73	−1.48	5.10
		132°04.51′W	50		30.76	−1.54	0.28
5	15 September	79°36.21′N	5	3800	27.27	−1.44	2.72
		146°50.63′W	37		30.89	−1.28	0.29
6	19 September	78°32.16′N	5	2450	30.14	−1.63	0.55
		124°57.08′W	60		31.48	−1.59	0.02
8	21 September	78°24.5′N	5	3650	26.62	−1.42	5.35
		134°35.2′W	30		29.12	−1.06	0.85
			70		31.06	−1.34	0.09
9	24 September	78°17.69′N	5	3800	26.98	−1.45	1.27
		140°56.22′W	45		30.79	−1.32	0.05
10	27 September	76°24.32′N	5	2770	27.52	−1.48	0.27
		131°7.58′W	55		31.04	−1.29	0.15
11	29 September	72°14.196′N	5	2990	23.15	0.40	1.31
		140°55.53′W	75		30.55	−0.69	0.03

Measurements from the CTD sensor.

mounting medium containing DAPI (Vector Laboratories, Inc., Burlingame, CA). Replicate counts for bacteria and fluorescent particle abundances used to calculate grazing impacts were determined with subsamples from each incubation bottle, fixed in 1% formalin and frozen at −20 °C until analysis. Bacteria were enumerated with fluorescence microscopy as described earlier and fluorescent particles counted by flow cytometry (FACSCalibur; BD Biosciences, San Jose, CA). Our experience was in agreement with Hyun & Yang (2003), who reported a minimum loss of bacterial cells kept frozen in this manner and counted within 2–3 months.

For feeding experiments, FLB or 0.6-μm polycarbonate microspheres (Polysciences, Inc., Warrington, PA) were added at approximately 25% of natural bacterial abundance. At Stations 1 and 2, FLB were the only tracers used. At Stations 3 and 4, FLB (1–1.2 μm) and microspheres (0.6 μm) were added to seawater in separate incubations. From these experiments, it was apparent that picoeukaryotes were not ingesting the larger FLB, and the use of FLB was discontinued in subsequent incubations. In all cases, fluorescent tracers were sonicated immediately prior to addition to disperse particles evenly. The replicate bottles were incubated at 2 °C under fluorescent lamps at irradiance levels between 2 and 7 × 10^{14} quanta s^{-1} cm^{-2}, depending on the depth from which the original samples were taken. Light level was measured with a QSL-100 Quantum-Scalar Irradiance meter (Biospherical Instruments, Inc., San Diego, CA). To determine rates of bacterivory, 100 mL aliquots were taken from the bottles at several time points beginning immediately after particle addition (T0) and fixed using the Lugol's/formaldehyde/$Na_2S_2O_3$ method to prevent egestion (Sherr & Sherr, 1993). After evaluation of initial time course data indicated linear uptake of both FLB and microspheres for 120 min, samples were taken at T0 (background correction) and 30 min to determine ingestion.

Ingestion rates and abundances of phototrophic, mixotrophic, and heterotrophic pico- and nanoplankton were determined from examination of 100 mL of sample filtered onto 25-mm Poretics polycarbonate membranes (3 μm pore size; GE Osmonics, Minnetonka, MN). Filters were simultaneously stained and mounted with cover slips on glass slides using VectaShield® as previously described for bacterial counts. To eliminate loss of chlorophyll fluorescence, specimens were frozen at −20 °C until enumeration by epifluorescence microscopy at 1000× magnification onboard the ship. Nanoplankton (3–20 μm) and picoeukaryotes ($\leq$ 2.5 μm) were counted in at least 25 fields per filter (a minimum of 100 and 200 cells for nanoplankton and picoplankton, respectively). Phototrophic and heterotrophic cells were differentiated by the presence or absence of chlorophyll autofluorescence, while mixotrophic cells were defined as those with chlorophyll and at least one ingested fluorescent tracer (FLB or microsphere) after background correction.

Statistical analysis of abundance and feeding data

To examine the potential for environmental factors to affect rates of bacterivory and proportions of mixotrophs, a Spearman's correlation analysis was performed using the statistical software program 'R' (Hornik, 2011); the arcsine transformation was used on percentage data prior to the analysis. ANOVA was used to test the effect of tracer particle (FLB, microsphere) on ingestion rates by HNAN and MNAN; relative feeding rates of MNAN and HNAN were examined with a paired comparisons method (Wilcoxon's signed ranks test). Statistical analysis of DGGE results is described in the following section.

Genetic analysis of samples

Twenty liters of water from the surface and DCM was collected directly from the Niskin bottles through 100-μm mesh prefilters onto 47-mm GF/F filters (Whatman) and frozen at −20 °C. Nucleic acids were recovered following the method described in Gast *et al.* (2004). One microlitre of each sample was amplified for DGGE analysis using the 18S rDNA primers 960FGC and 1200R, generating a *c.* 250-bp fragment from the V7 region following the method described in Gast *et al.* (2004). Triplicate PCR products were precipitated and resuspended in a total of 6 μL of sterile distilled water. Nucleic acid concentrations were estimated with a Nanodrop™ 1000 (Thermo Fisher Scientific, Waltham, MA), and about 500 ng of each sample was loaded onto the gradient gel, which was poured and run following the procedure in Gast *et al.* (2004). The image was analyzed using GELCOMPARII (Applied Maths, Austin, TX), and bands detected manually were scored by presence/absence with a tolerance of 1%. Diversity and environmental factors were analyzed using PERMANOVA+ (Anderson *et al.*, 2008). The DGGE band data matrix was converted to a Bray–Curtis-based resemblance matrix, with the environmental factors of site (each station) and depth (surface and deep). Environmental variables included actual depth, site, temperature, photosynthetically active radiation (PAR), Julian date, and salinity. An analysis of variance was performed with PERMANOVA+, and principal coordinates analysis (PCO) was used to visualize the diversity patterns related to environmental variables.

Well-separated bands were picked from the gel using a sterile pipet tip to touch the surface of the gel and then pipetting up and down in 5 μL of sterile distilled water. In our experience, this method has reduced the recovery of multiple bands that occurs when cutting a band from the gel and eluting material from the matrix. The band was reamplified from 2.5 μL of the sample with the non-GC clamped primer set. Samples were precipitated overnight at −20 °C with a final concentration of 0.3 M sodium acetate and 0.6 volumes of 100% isopropanol. They were resuspended in 5 μL of water, and 250 ng were sequenced at the Bay Paul facility (MBL) using the non-GC clamped forward primer (960f). Putative band sequence identities were assessed using BLAST™ (GenBank), and we did not observe any potentially chimeric sequences. GenBank no longer accepts sequences shorter than 200 bp, and because six of ours are below this limit, we have made our sequence data available in the Supporting Information (Table S1).

Results

General environmental parameters

The surface salinities and temperatures observed in the Beaufort Sea and the Canada Basin during the study period ranged from 23.15 to 31.49 PSU and −1.63 to 0.4 °C, respectively (Table 1). PAR measured at the time of sampling ranged from 0.27 to 5.35 quanta cm^{-2} s^{-1} × 10^{15} at the surface, but never exceeded 0.29 quanta cm^{-2} s^{-1} × 10^{15} at the chlorophyll maximum depth of any station (Table 1). The general oceanographic parameters of salinity, temperature, and light (Table 1) are within the range of previous reports for the region and the season (Cota *et al.*, 1996; Lovejoy *et al.*, 2007; Sherr *et al.*, 2009; Tremblay *et al.*, 2009).

Plankton abundances

Overall, abundances of microorganisms were low, as expected for the region and the autumn season. Bacteria were typically present at between 1 and 2 × 10^5 cells mL^{-1} (Table 2). The maximum chlorophyll *a* concentration, observed at the DCM of Station 1, was 0.87 μg L^{-1} (Table 2). The abundance of phytoplankton reflected the low chlorophyll concentrations. Diatoms were conspicuously absent from most samples and had a maximum abundance of < 1 mL^{-1}. Dinoflagellates were present in all samples, and although the Lugol's-fixed samples used for microplankton enumeration did not enable differentiation between phototrophic and purely heterotrophic individuals, qualitative shipboard observations with epifluorescence microscopy indicated that heterotrophic dinoflagellates tended to be more abundant than phototrophic dinoflagellates by a factor of 2 : 1 to 3 : 1. The combined dinoflagellates always numerically dominated the other microflagellates, with a maximum of approximately 7 mL^{-1} (Table 2). Ciliate abundances frequently mirrored the 'other microflagellate' category and exceeded 2 mL^{-1} on only two occasions at the surface.

Table 2. Station microbial characteristics. Chlorophyll *a* concentration (μg L^{-1}), heterotrophic and autotrophic microplankton abundance (no. mL^{-1}), and bacterial abundance (× 10^5 mL^{-1}) in the Beaufort Sea

Station	Depth (m)	Chl *a*	Ciliates	Dino-flagellates	Other flagellates	Centric diatoms	Pennate diatoms	Bacteria
1	5	0.16	0.51	2.54	*	*	0.20	5.50
	60	0.87	0.91	3.86	*	0.30	0.20	–
2	5	0.20	0.25	2.85	2.85	*	*	2.20
	50	0.51	0.44	4.50	0.19	0.06	*	1.81
3	5	0.29	2.03	7.25	0.25	*	0.10	1.80
	50	0.42	0.36	2.18	0.30	*	*	2.20
4	5	0.28	2.22	5.71	1.84	*	0.25	2.49
	50	0.30	0.41	3.25	0.86	*	0.05	1.93
5	5	0.44	1.78	7.00	1.42	*	0.10	1.70
	37	0.54	1.37	5.68	1.83	*	0.05	1.98
6	5	0.20	0.36	1.37	0.41	*	*	1.84
	60	0.35	0.91	2.43	0.71	*	*	2.18
8	5	0.26	1.22	5.17	0.30	0.05	*	1.33
	30	0.29	0.36	2.23	*	*	*	1.17
	70	0.34	0.10	2.33	0.20	*	*	1.60
9	5	0.24	1.07	5.88	1.62	0.05	*	1.65
	45	0.40	0.51	3.25	0.81	*	*	1.37
10	5	0.23	0.91	2.94	1.12	*	*	1.31
	55	0.30	0.20	2.33	0.61	*	*	2.51
11	5	0.22	1.32	4.26	0.71	*	*	1.65
	75	0.28	0.41	1.62	0.30	0.10	*	1.24

*Not observed.

Heterotrophic (HNAN) and phototrophic nanoflagellates (PNAN), mostly in the 4–6 μm size range, were typically present at 50–200 cells mL^{-1}, while MNAN abundances were usually at 5–20 cells mL^{-1} (Table 3). Photosynthetic picoeukaryotes (Peuk) were the numerically dominant group, and usually exceeded 10^3 cells mL^{-1} (Table 3). Mixotrophic picoeukaryotes (Mpeuk) were identified at every station after the switch was made to smaller (0.6 μm) tracer particles. The abundances of Mpeuk usually exceeded that of the MNAN, sometimes by an order of magnitude (Table 3). However, they made up only a very small proportion of the total picoeukaryotes, while MNAN comprised up to 32% of the PNAN (Table 3). MNAN should also be compared with HNAN because both contribute to grazing impact on bacteria. MNAN were on average 10% (range 1–22%) of the bacterivorous nanoplankton (Table 3).

Ingestion rates and bacterivory impact

Time courses run at the beginning of the cruise indicated that uptake of both FLB and microspheres were linear for the first 120 min of incubation, after which ingestion was balanced by digestion and egestion. At Stations 1 and 2, only FLB were used as tracer particles, but at Stations 3 and 4, separate feeding experiments were run with the same communities using either FLB or fluorescent microspheres. Grazing rates by nanoflagellates were greater on microspheres than on FLB in cases where both tracer types were used (Table S2), and ingestion by Mpeuks was detected only in experiments with microspheres. At Stations 3 and 4 where direct comparisons were made, average calculated ingestion rates using microsphere tracers were 0.9 and 3.3 bacteria per individual per hour for HNAN and MNAN, respectively. Using FLB, the corresponding rates were 0.2 and 2.2 bacteria per individual per hour. The ingestion rates determined using microspheres were significantly greater than those determined with FLB for both HNAN and MNAN (ANOVA, $P < 0.01$). Polar bacteria tend to be < 1 μm in size, and the higher rates observed for ingestion of microspheres may reflect size-selective feeding, although larger sized particle ingestion still occurred for the nanoplankton.

Grazing rates were not consistently affected by depth (surface vs. DCM). For all three grazing groups, ingestion was greater in surface waters than at the DCM about half the time. Rates were greater in the DCM only twice for HNAN and MNAN and only once for Mpeuk. For the remainder of the incubations, there was no significant difference between depths. Over all experiments, the calculated individual grazing rates were greater for MNAN than for HNAN ($P < 0.001$, Table S2). Using microsphere tracers, the average ingestion rates for HNAN and MNAN were 1.3 and 5.1 bacteria per individual per hour, respectively. For Mpeuk, the average ingestion rate (from microsphere incubations) was 2.9 bacteria per individual per hour. The reported ingestion rates per cell for MNAN

Table 3. Abundances (no. mL^{-1} ± SE) of HNAN, PNAN, MNAN, photosynthetic picoeukaryotes (Peuk) and mixotrophic picoeukaryotes (Mpeuk), and mixotrophs as a percentage of all similarly sized phototrophs and heterotrophs. Picoeukaryotes did not ingest FLB, and microspheres were not used until Station 3. Note that the percentage calculations include mixotrophs as part of the total nano- and picoplankton abundance

Station	Depth (m)	HNAN	PNAN	MNAN	Peuk	Mpeuk	% of PNAN	% of HNAN	% of Peuk
1	5	93 ± 5	25 ± 4	7 ± 1	–	–	21	7	–
2	5	45 ± 6	15 ± 5	2 ± 1	–	–	13	5	–
	50	23 ± 4	82 ± 8	3 ± 0	–	–	4	12	–
3	5	66 ± 15	71 ± 6	11 ± 3	1217 ± 164	30 ± 5	14	15	2
	50	52 ± 10	48 ± 17	5 ± 1	872 ± 283	18 ± 4	9	9	2
4	5	90 ± 3	54 ± 5	3 ± 1	1901 ± 108	56 ± 22	5	3	3
	50	57 ± 15	34 ± 3	16 ± 1	880 ± 45	6 ± 6	32	22	1
5	5	121 ± 30	46 ± 11	19 ± 2	2757 ± 242	220 ± 16	30	14	7
	37	143 ± 20	77 ± 22	16 ± 6	2807 ± 251	155 ± 17	17	10	5
6	5	129 ± 13	97 ± 17	36 ± 3	444 ± 77	9 ± 5	27	22	2
	60	126 ± 23	143 ± 35	22 ± 8	324 ± 59	18 ± 6	13	15	5
8	5	130 ± 12	45 ± 5	8 ± 4	3021 ± 310	87 ± 3	15	6	3
	30	102 ± 10	126 ± 18	10 ± 5	1598 ± 54	61 ± 2	8	9	4
	70	108 ± 21	91 ± 10	5 ± 1	952 ± 101	4 ± 3	5	4	< 1
9	5	206 ± 36	106 ± 9	2 ± 1	3047 ± 695	139 ± 7	2	1	4
	47	178 ± 13	100 ± 7	19 ± 3	1523 ± 123	77 ± 4	16	10	5
10	5	97 ± 26	51 ± 18	8 ± 3	1862 ± 290	12 ± 6	13	8	1
	55	114 ± 9	65 ± 4	2 ± 2	914 ± 278	16 ± 6	3	2	2
11	5	193 ± 7	45 ± 11	13 ± 1	2011 ± 208	0	22	6	< 1
	75	66 ± 6	25 ± 12	7 ± 3	1061 ± 161	25 ± 18	23	10	2

and Mpeuk are inflated relative to those of HNAN because of the method of calculation. HNAN that do not ingest tracers during an experiment can be counted, while potential mixotrophs that are 'inactive grazers' usually cannot be distinguished from pure autotrophs. Therefore, the total number of mixotrophs is based only on those ingesting tracers. This does not, however, affect the relative grazing impacts (see discussion).

The potential grazing impact of protists on bacteria ranged from < 1% to 25.2% of bacterial standing stock per day; the impact was < 5% of standing stock per day in 15 of 20 incubations (Table S3). HNAN, frequently identified as the major planktonic bacterivores, dominated the grazing impact in about half of the experiments, while mixotrophs were more important in the rest (Fig. 2). Mpeuks tended to dominate bacterivory in experiments where the highest total impacts were determined (Table S3). Regarding correlations between ingestion rates and environmental parameters, HNAN rates were positively correlated to light, but there were no other significant relationships (Table S4). MNAN as a proportion of total nanoplankton bacterivores (MNAN/[MNAN + HNAN]) was negatively correlated to salinity and positively correlated to light. Mpeuk as a proportion of Peuk was positively correlated to chlorophyll *a*, dinoflagellates, and total Peuk abundance.

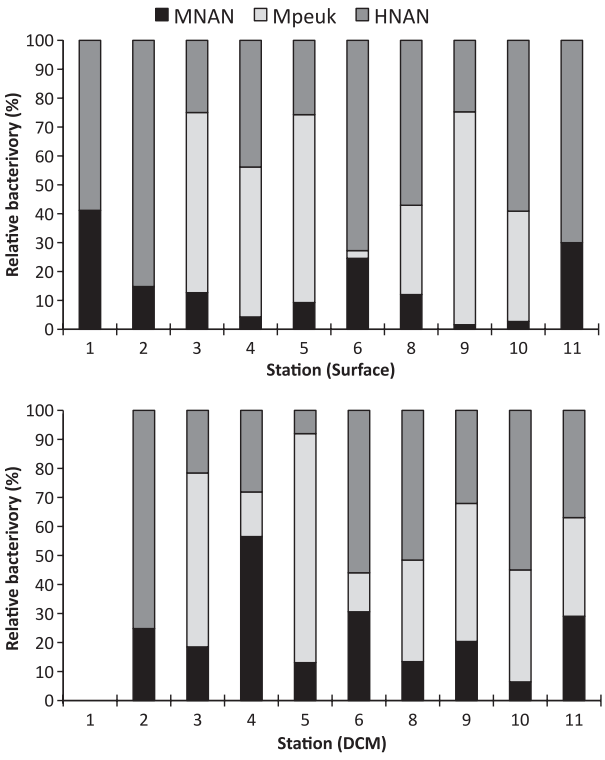

Fig. 2. Relative impact of MNAN, mixotrophic picoeukaryotes (Mpeuk), and HNAN as grazers of bacterioplankton.

Community structure and comparison

The DGGE results are shown in Fig. 3, with the bands successfully recovered for sequencing numbered in panels A and B, and the PCO results in panel C. Generally, there were fewer than five predominant bands in each sample that were possible to recover for sequencing. Many more were identifiable for community analysis using GelComparII (Applied Maths). Taxonomic affiliation of DGGE band sequences was determined using Blast™. Sequences recovered include dinoflagellates, diatoms, copepods, dinoflagellate parasites (Syndiniales), and *Micromonas* (a mixotrophic picoeukaryote), with bands from the same position in different samples giving the same sequence results (Table S5). Permanova+ indicated that both depth ($P = 0.0086$) and location ($P = 0.0001$) were significant in describing the diversity between samples, but that there was no synergistic interaction between the factors ($P = 0.7085$). Site and date variables were colinear, so date was removed from further analyses. The PCO analysis illustrated the effect of site/date and depth on the grouping of samples (Fig. 3c). Separation of two groups along the first axis corresponded to the midpoint of the cruise and described 28.8% of the total variation. The second axis described slightly less of the overall variation (19.3%) and appeared to correspond to depth.

Discussion

Protists play important roles as both primary producers and consumers in southern and northern polar waters (Sherr *et al.*, 2003; Riedel *et al.*, 2007; Pearce *et al.*, 2010). However, previous to the current investigation, nothing was known about mixotrophic protists in the Arctic. Our study confirms the presence of both nano- and picoplanktonic mixotrophs in the Arctic Ocean, and their potential for substantial impact on bacterial communities

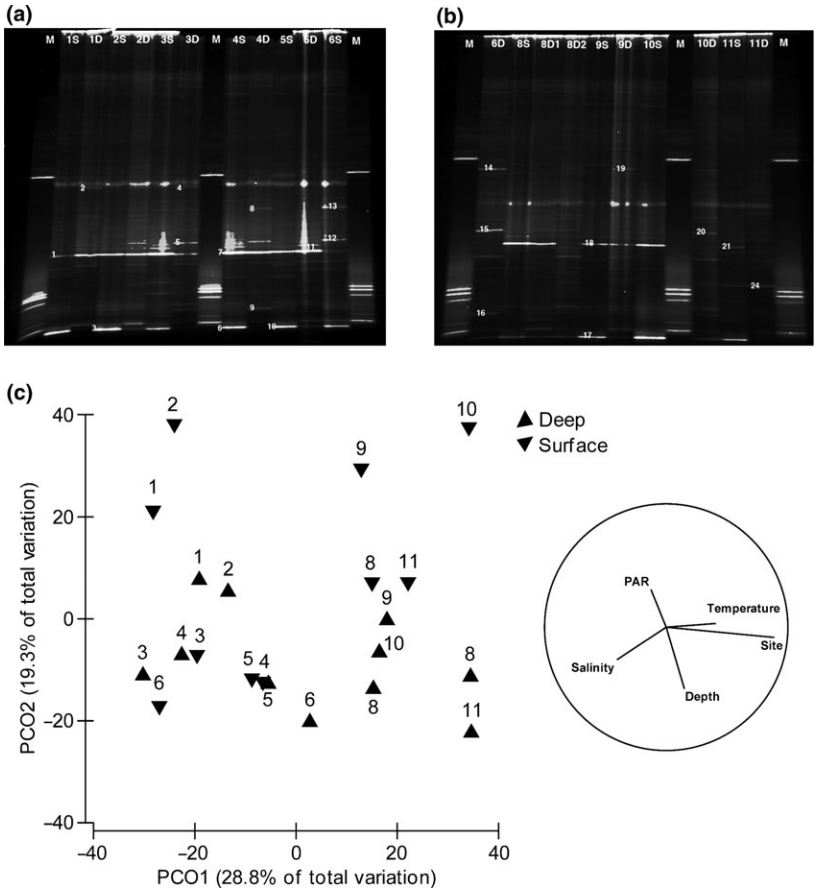

Fig. 3. DGGE results from the Beaufort Sea and the Canada Basin. (a) Samples from Stations 1–6 and (b) samples from Stations 6–11 (numbers indicate band successfully recovered and sequenced). (c) PCO plot with environmental variable vectors at the right; deep = DCM, surface = 5 m, numbers indicate each station. Axis 1 represents 28.8% of the total variation, while axis 2 represents 19.3% of the total. These appear to represent the variables of site/location and depth respectively.

in the ice-covered Arctic region of the Beaufort Sea in early autumn.

Protistan abundance

Our microscopic investigation of bacterial and protist distribution indicated that densities were low, but within the range of previous reports for the Canada Basin and Beaufort Sea during the late summer to early fall (Table 4). Picophytoplankton were the most abundant protists, typically outnumbering hetero- and autotrophic nanoplankton by an order of magnitude (Table 3). A small percentage of the picoeukaryotes, from < 1% to 7%, were identified as mixotrophic by ingestion of fluorescent tracers, but at most stations, they were still more abundant than MNAN identified in the same manner (Table 3). At least one cultured strain of the picoprasinophyte *Micromonas* was previously found to be phagotrophic (González *et al.*, 1993), and most of the mixotrophic picoeukaryotes enumerated with epifluorescence microscopy in our study resembled the 'typical *Micromonas*-like cell stained with DAPI' as presented in a color photomicrograph in Lovejoy *et al.* (2007). Coupled with the frequent occurrence of bands in the DGGE gels that were linked to *Micromonas* (Fig. 3, Table S5), our data indicate potential for relatively large impacts by this picoprasinophyte as a bacterivore in the Arctic ecosystem at this time. Furthermore, the wide-spread occurrence of *Micromonas* (Sherr *et al.*, 2003; Not *et al.*, 2005; Lovejoy *et al.*, 2007; Tremblay *et al.*, 2009) suggests that mixotrophy could be common in the Arctic throughout the year.

After picoplankton, HNAN were the next most numerous protists, although HNAN abundance was usually within a factor of two of combined PNAN and MNAN assemblages. Sherr *et al.* (1997) also found that < 5 μm HNAN were numerically dominant heterotrophs, but noted that the 6 to 20-μm-size class tended to dominate heterotrophic biomass in integrated samples (0–50 m) along a cruise track from the Chukchi Sea to the Nansen Basin from July through August (Sherr *et al.*, 1997; Wheeler *et al.*, 1997). The microplankton size-fraction in our samples was always dominated by dinoflagellates and ciliates, although abundances were on the low end of ranges reported previously for arctic and subarctic waters (Sherr *et al.*, 1997; Levinsen *et al.*, 2000; Strom *et al.*, 2007; Vaqué *et al.*, 2008). Diatoms were observed at very low abundances, if at all, in our microscope counts (Table 2). Likewise, Sherr *et al.* (2003) reported Arctic Ocean winter diatom abundances $\leq$ 1 cell mL^{-1}, and Terrado *et al.* (2009) reported diatoms represented only 4% of autumn clone library sequences in Franklin Bay.

Table 4. Abundances of microorganisms reported from Arctic waters

Location	Dates	Bacteria (no. mL^{-1})	Synecho (no. mL^{-1})	HNAN (no. mL^{-1})	Peuk (no. mL^{-1})	PNAN (no. mL^{-1})	Ciliates (no. mL^{-1})	Dinoflag (no. mL^{-1})
S. Canada Basin (Sherr *et al.*, 2003)	November 1997–May 1998	1–3 × 10^5		90–490	'hundreds'	3–1500	0.1–2	1–12
Beaufort Sea/NW Passage (Lovejoy *et al.*, 2007)	February–May 2004				10–9500			
Canadian Arctic/Franklin Bay (Vaqué *et al.*, 2008)	December 2003–May 2004	1–5 × 10^5		200–600		30–450	0.1–1.3	
Central Arctic (Booth & Horner, 1997)	July–September 1994				1000–10 000	42–910		9–105
Central Arctic (Sherr *et al.*, 1997; pooled from upper 50 m, same cruise as Booth & Horner, 1997)	July–September 1994	4–12 × 10^5	Not observed	250–1900	1000–10 000	Not reported	0.1–17	0.1–39
Chukchi Plateau/Mendeleyev Basin (Sherr *et al.*, 2003)	June–September 1998	2–7 × 10^5		210–2300	1000–28 000	100–28 000	0.1–2	1–12
North Baffin Bay (Tremblay *et al.*, 2009)	August–September 2005		0–17		660–10 365			
NW Passage (Tremblay *et al.*, 2009)	August–September 2005		1–70		860–18 360			
Beaufort Sea/Amundsen Gulf (Tremblay *et al.*, 2009)	August–September 2005		1–120		150–16 990			
North Baffin Bay (Mostajir *et al.* 2001)	September–October 1999				18–4070	130–3080		
Mackenzie Shelf/Amundsen Gulf (Waleron *et al.* 2007)	September–October 2002		470–2425		215–2110			
Beaufort Sea/Canada Basin (This study)	September 2008	1–5 × 10^5	Not observed	20–200	320–3050	15–140	0.2–2.2	1–7

Synecho, *Synechococcus* spp.; Peuk, picoeukaryotes; Dinoflag, dinoflagellates.

Protistan diversity

Low biomass as indicated by the microscopic and pigment observations would not necessarily indicate low diversity. However, microscopy suggested that only a limited number of taxa were present, with diatoms absent from most samples. DGGE also yielded only a few predominant bands for each sample, although many faint bands were also present.

When the recovered Arctic DGGE bands were compared with those recovered from the Antarctic (Gast *et al.*, 2004) at a level of 97% similarity, the only overlap in sequence information was for the copepod *Oithona*. Prior genetic studies of microbial eukaryotes in the Arctic have used both DGGE and clone libraries to examine the community structure (Lovejoy *et al.*, 2006; Hamilton *et al.*, 2008; Terrado *et al.*, 2009; Tremblay *et al.*, 2009; Bachy *et al.*, 2011; Lovejoy & Potvin, 2011). The DGGE fragment used in this study targeted a different region of the ribosomal gene than some of those projects, and most of those studies have been directed toward the < 5-μm size group, yet there are similarities. The groups commonly identified by molecular diversity surveys of Arctic waters included alveolates (ciliates, dinoflagellates, and group I & II alveolates), unidentified marine stramenopile genotypes (MAST), dictyophytes, prasinophytes, haptophytes, diatoms, bolidophytes, cryptophytes, and the newly identified picobiliphytes. In common with this work, other studies have also reported the abundance and wide distribution of *Micromonas* (Sherr *et al.*, 2003; Lovejoy *et al.*, 2007; Terrado *et al.*, 2008), as well as the diatom *Chaetoceros*, novel alveolate group II Syndiniales, and other dinoflagellates.

Mixotrophy, bacterivory, and grazing impacts

The ubiquitous occurrence of mixotrophic plankton found in this study and in a recent reports from Antarctic waters (Moorthi *et al.*, 2009) suggests that mixotrophy may be a successful strategy for some phytoplankton in polar marine environments. The potential benefits of particle ingestion by phytoplankton include the acquisition of organic carbon, energy, major nutrients, and/or micronutrients including vitamins and trace metals (e.g. Caron *et al.*, 1993; Nygaard & Tobiesen, 1993; Maranger *et al.*, 1998). If, as has been suggested by Tremblay & Gagnon (2009), primary production in seasonally ice-free waters of the Arctic Ocean is controlled by nitrogen supply, then mixotrophy there may act as a competitive mechanism for nitrogen uptake. Increased mixotrophy under nutrient limitation has been noted for nanoplankton and suggested for picoeukaryotes in other marine systems (Nygaard & Tobiesen, 1993; Zubkov & Tarran, 2008), although the environmental drivers of mixotrophic behavior are likely to vary with species.

In the Ross Sea Antarctica, photosynthetic and HNAN range over three orders of magnitude from about 2 mL^{-1} to 7×10^3 mL^{-1} and peak in austral summer (Dennett *et al.*, 2001; Moorthi *et al.*, 2009). MNAN were typically < 200 mL^{-1} in plankton assemblages south of the Polar Front of the Southern Ocean, but still comprised 8–42% of bacterivorous nanoplankton in the water column, and 5–10% of phototrophic and 3–15% of phagotrophic nanoflagellates present in ice cores (Moorthi *et al.*, 2009). The abundance of MNAN during the Arctic autumn ranged from 2 to 300 mL^{-1} and comprised the same relative abundances when compared to total heterotrophic (1–22%) and total phototrophic (2–32%) nanoplankton (Table 3) as was observed during austral summer. A major difference in our studies of mixotrophs in the Arctic and Southern Oceans was the abundance and impact of the picophytoplankton. While phototrophic picoeukaryotes were not noted in our Antarctic samples, they numerically dominated many of the Arctic samples and were important as bacterivores.

Food size appeared to be of consequence for the mixotrophic picoeukaryotes; ingestion was observed when the 0.6-μm microspheres were used, but never when the 1–1.2 μm FLB were offered. Grazing by nanoflagellates on microspheres also was significantly greater than on FLB ($P < 0.001$, ANOVA), although absolute differences were not large. Overall, the mixotrophic community (MNAN and Mpeuks) ingested 2× as many bacteria-sized particles as the heterotrophs, indicating that they had an equivalent or greater grazing impact on bacteria as that of the more traditional (heterotrophic) consumer population.

As a community, the pico- and nanoplankton removed from 0.06 to 2.6×10^4 bacteria mL^{-1} day^{-1}, dependent to a large degree on the abundance of picoeukaryotes. This compares to a grazing impact, estimated using FLB, of 0.1–4.6×10^4 bacteria mL^{-1} day^{-1} by heterotrophic plankton during the Arctic summer (Sherr *et al.*, 1997). Anderson & Rivkin (2001) used the dilution technique to examine bacterivory, and also noted significant grazing impact during early summer blooms and during winter in Resolute Bay, Northwest Territories, Canada.

This is the first study to demonstrate mixotrophy by phytoflagellates in Arctic waters, and the data suggest that a *Micromonas*-like picoprasinophyte was an important bacterivore in the Canada Basin during autumn. The role of picoeukaryotes as quantitatively important grazers has been demonstrated only once previously – in the North Atlantic Ocean (Zubkov & Tarran, 2008), although it was conjectured to occur in the Arctic (Sherr *et al.*, 2003). As these picoprasinphytes are known to persist through winter darkness and grow exponentially from late winter to early spring (Lovejoy *et al.*, 2007), phagotrophy may

contribute importantly to survival during winter darkness and give the organisms a relatively large seed population at the beginning of the spring growth period. If global climate change freshens the Arctic Ocean as proposed by Li *et al.* (2009), the impact of picoeukaryotes as bacterivores may become especially important.

Acknowledgements

We gratefully acknowledge the captain and crew of *US-CGC Healy* for logistical support, and the United State Geological Survey (Woods Hole, MA and Menlo Park, CA) for allowing us to participate in the HLY0806 cruise. Funding for participation in the 2008 cruise was provided by the Woods Hole Oceanographic Institution Arctic Research Initiative, with additional support from National Science Foundation Grants OPP-0838847 (R.W.S.) and OPP-0838955 (R.J.G.). We thank Zaid McKee-Krisberg and Scott Fay, respectively, for assistance with R statistical software and Generic Mapping Tools (GMT) used to create Fig. 1.

Authors' contribution

R.W.S. and R.J.G. contributed equally to this paper.

References

Anderson MR & Rivkin RB (2001) Seasonal patterns in grazing mortality of bacterioplankton in polar oceans: a bipolar comparison. *Aquat Microb Ecol* **25**: 195–206.

Anderson MJ, Gorely RN & Clarke KR (2008) *Permanova+ for Primer: Guide to Software and Statistical Methods*. Primer-E, Ltd, Plymouth, UK.

Bachy C, Lopez-Garcia P, Vereshchaka A & Moreira D (2011) Diversity and vertical distribution of microbial eukaryotes in the snow, sea ice and seawater near the North Pole at the end of the polar night. *Front Microbiol* **2**: 106. doi: 10.3389/fmicb.2011.00106.

Bell EM & Laybourn-Parry J (2003) Mixotrophy in the Antarctic phytoflagellate, *Pyramimonas gelidicola* (Chlorophyta: Prasinophyceae). *J Phycol* **39**: 644–649.

Booth BC & Horner RA (1997) Microalgae on the arctic ocean section, 1994: species abundance and biomass. *Deep Sea Res Part 2 Top Stud Oceanogr* **44**: 1607–1622.

Caron DA, Sanders RW, Lim EL, Marrasé C, Amaral LA, Whitney S, Aoki RB & Porter KG (1993) Light-dependent phagotrophy in the freshwater mixotrophic chrysophyte *Dinobryon cylindricum*. *Microb Ecol* **25**: 93–111.

Cota GF, Pomeroy LR, Harrison WG, Jones EP, Peters F, Sheldon J, W.M. & Weingartner TR (1996) Nutrients, primary production and microbial heterotrophy in the southeastern Chukchi Sea: Arctic summer nutrient depletion and heterotrophy. *Mar Ecol Prog Ser* **135**: 247–258.

Dennett MR, Mathot S, Caron DA, Smith WO Jr & Lonsdale DJ (2001) Abundance and distribution of phototrophic and heterotrophic nano- and microplankton in the southern Ross Sea. *Deep Sea Res Part 2 Top Stud Oceanogr* **48**: 4019–4037.

Gast RJ, Dennett MR & Caron DA (2004) Characterization of protistan assemblages in the Ross Sea, Antarctica, by denaturing gradient gel electrophoresis. *Appl Environ Microbiol* **70**: 2028–2037.

González JM, Sherr BF & Sherr EB (1993) Digestive enzyme activity as a quantitative measure of protistan grazing: the acid lysozyme assay for bacterivory. *Mar Ecol Prog Ser* **100**: 197–206.

Hamilton AK, Lovejoy C, Galand PE & Ingram RG (2008) Water masses and biogeography of picoeukaryote assemblages in a cold hydrographically complex system. *Limnol Oceanogr* **53**: 922–935.

Havskum H & Hansen AS (1997) Importance of pigmented and colourless nano-sized protists as grazers on nanoplankton in a phosphate-depleted Norwegian fjord and in enclosures. *Aquat Microb Ecol* **12**: 139–151.

Havskum H & Riemann B (1996) Ecological importance of bacterivorous, pigmented flagellates (mixotrophs) in the Bay of Aarhus, Denmark. *Mar Ecol Prog Ser* **137**: 251–263.

Hornik K (2011) The R FAQ. Available at: http://CRAN.R-project.org/doc/FAQ/.

Hyun J-H & Yang E-J (2003) Freezing seawater for the long-term storage of bacterial cells for microscopic enumeration. *J Microbiol* **41**: 262–265.

Jeong HJ (2011) Mixotrophy in red tide algae raphidophytes. *J Eukaryot Microbiol* **58**: 215–222.

Jeong HJ, Yoo YD, Kim JS, Seong KA, Kang NS & Kim TH (2010) Growth, feeding and ecological roles of the mixotrophic and heterotrophic dinoflagellates in marine planktonic food webs. *Ocean Sci J* **45**: 65–91.

Levinsen H, Nielsen TG & Hansen BW (2000) Annual succession of marine pelagic protozoans in Disko Bay, West Greenland, with emphasis on winter dynamics. *Mar Ecol Prog Ser* **206**: 119–134.

Li WKW, McLaughlin FA, Lovejoy C & Carmack EC (2009) Smallest algae thrive as the Arctic Ocean freshens. *Science* **326**: 539.

Lovejoy C & Potvin M (2011) Microbial eukaryotic distribution in a dynamic Beaufort Sea and the Arctic Ocean. *J Plankton Res* **33**: 431–444.

Lovejoy C, Massana R & Pedrós-Alió C (2006) Diversity and distribution of marine microbial eukaryotes in the Arctic Ocean and adjacent seas. *Appl Environ Microbiol* **72**: 3085–3095.

Lovejoy C, Vincent WF, Bonilla S, Roy S, Martineau M-J, Terrado R, Potvin M, Massana R & Pedrós-Alió C (2007) Distribution, phylogeny, and growth of cold-adapted picoprasinophytes in Arctic seas. *J Phycol* **43**: 78–89.

Maranger R, Bird DF & Price NM (1998) Iron acquisition by photosynthetic marine phytoplankton from ingested bacteria. *Nature* **396**: 248–251.

Moorthi S, Caron DA, Gast RJ & Sanders RW (2009) Mixotrophy: a widespread and important ecological strategy for planktonic and sea-ice nanoflagellates in the Ross Sea, Antarctica. *Aquat Microb Ecol* **54**: 269–277.

Mostajir B, Gosselin M, Gratton Y, Booth B, Vasseur C, Garneau M-È, Fouilland É, Vidussi F & Demers S (2001) Surface water distribution of pico- and nanophytoplankton in relation to two distinctive water masses in the North Water, northern Baffin Bay, during fall. *Aquat Microb Ecol* **23**: 205–212.

Not F, Massana R, Latasa M, Marie D, Colson C, Eikrem W, Pedrós-Alió C, Vaulot D & Simon N (2005) Late summer community composition and abundance of photosynthetic picoeukaryotes in Norwegian and Barents seas. *Limnol Oceanogr* **50**: 1677–1686.

Nygaard K & Tobiesen A (1993) Bacterivory in algae: a survival strategy during nutrient limitation. *Limnol Oceanogr* **38**: 273–279.

Pearce I, Davidson AT, Thomson PG, Wright S & van den Enden R (2010) Marine microbial ecology off East Antarctica (30–80∞E): rates of bacterial and phytoplankton growth and grazing by heterotrophic protists. *Deep Sea Res Part 2 Top Stud Oceanogr* **57**: 849–862.

Riedel A, Michel C & Gosselin M (2007) Grazing of large-sized bacteria by sea-ice heterotrophic protists on the Mackenzie Shelf during the winter–spring transition. *Aquat Microb Ecol* **50**: 25–38.

Sanders RW (2011) Alternative nutritional strategies in protists: symposium introduction and a review of freshwater protists that combine photosynthesis and heterotrophy. *J Eukaryot Microbiol* **58**: 181–184.

Sanders RW & Porter KG (1988) Phagotrophic phytoflagellates. *Advances in Microbial Ecology*, Vol. 10 (Marshall KC, eds), pp. 167–192. Plenum, New York.

Sanders RW, Porter KG, Bennett SJ & DeBiase AE (1989) Seasonal patterns of bacterivory by flagellates, ciliates, rotifers, and cladocerans in a freshwater planktonic community. *Limnol Oceanogr* **34**: 673–687.

Sanders RW, Berninger U-G, Lim EL, Kemp PF & Caron DA (2000) Heterotrophic and mixotrophic nanoplankton predation on picoplankton in the Sargasso Sea and on Georges Bank. *Mar Ecol Prog Ser* **192**: 103–118.

Sherr EB & Sherr BF (1993) Protistan grazing rates via uptake of fluorescently labeled prey. *Handbook of Methods in Aquatic Microbial Ecology* (Kemp PF, Sherr BF, Sherr EB & Cole JJ, eds), pp. 695–701. Lewis Publishers, Boca Raton, FL.

Sherr EB, Sherr BF & Fessenden L (1997) Heterotrophic protists in the central Arctic Ocean. *Deep Sea Res Part 2 Top Stud Oceanogr* **44**: 1665–1682.

Sherr EB, Sherr BF, Wheeler PA & Thompson K (2003) Temporal and spatial variation in stocks of autotrophic and heterotrophic microbes in the upper water column of the central Arctic Ocean. *Deep Sea Res Part 1 Oceanogr Res Pap* **50**: 557–571.

Sherr EB, Sherr BF & Hartz AJ (2009) Microzooplankton grazing impact in the Western Arctic Ocean. *Deep Sea Res Part 2 Top Stud Oceanogr* **56**: 1264–1273.

Stoecker DK, Johnson MD, deVargas C & Not F (2009) Acquired phototrophy in aquatic protists. *Aquat Microb Ecol* **57**: 279–310.

Strom SL, Macri EL & Olson MB (2007) Microzooplankton grazing in the coastal Gulf of Alaska: variations in top–down control of phytoplankton. *Limnol Oceanogr* **52**: 1480–1494.

Terrado R, Lovejoy C, Massana R & Vincent WF (2008) Microbial food web responses to light and nutrients beneath the coastal Arctic Ocean sea ice during the winter-spring transition. *J Mar Syst* **74**: 964–977.

Terrado R, Vincent WF & Lovejoy C (2009) Mesopelagic protists: diversity and succession in a coastal Arctic ecosystem. *Aquat Microb Ecol* **56**: 25–40.

Tremblay J-É & Gagnon J (2009) The effects of irradiance and nutrient supply on the productivity of Arctic waters: a perspective on climate change. *Influence of Climate Change on the Changing Arctic and Sub-Arctic Conditions* (Nihoul JCJ & Kostianoy AG, eds), pp. 73–93. Springer, Dordrecht, the Netherlands.

Tremblay G, Belzile C, Gosselin M, Poulin M, Roy S & Tremblay J-É (2009) Late summer phytoplankton distribution along a 3500 km transect in Canadian Arctic waters: strong numerical dominance by picoeukaryotes. *Aquat Microb Ecol* **54**: 55–70.

Unrein F, Massana R, Alonso-Sáez L & Gasol JM (2007) Significant year-round effect of small mixotrophic flagellates on bacterioplankton in an oligotrophic coastal system. *Limnol Oceanogr* **52**: 456–469.

Vaqué D, Guadayol Ò, Peters F, Felipe J, Angel-Ripoll L, Terrado R, Lovejoy C & Pedrós-Alió C (2008) Seasonal changes in planktonic bacterivory rates under the ice-covered coastal Arctic Ocean. *Limnol Oceanogr* **53**: 2427–2438.

Waleron M, Waleron K, Vincent WF & Wilmotte A (2007) Allochthonous inputs of riverine picocyanobacteria to coastal waters in the Arctic Ocean. *FEMS Microbiol Ecol* **59**: 356–365.

Wheeler PA, Watkins JM & Hansing RL (1997) Nutrients, organic carbon and organic nitrogen in the upper water column of the Arctic Ocean: implications for the sources of dissolved organic carbon. *Deep Sea Res Part 2 Top Stud Oceanogr* **44**: 1571–1592.

Zubkov MV & Tarran GA (2008) High bacterivory by the smallest phytoplankton in the North Atlantic Ocean. *Nature* **455**: 224–226.

Supporting Information

Additional Supporting Information may be found in the online version of this article:

Table S1. Sequence data for DGGE bands identified in Fig. 3 of Sanders and Gast.

Table S2. Ingestion rates (bacteria protist^{-1} h^{-1} ± SE) of heterotrophic nanoflagellates (HNAN), phototrophic nano-

flagellates (PNAN), mixotrophic nanoflagellates (MNAN), and mixotrophic picoeukaryotes (Mpeuk).

Table S3. Protistan grazing impact as a percentage of bacteria standing stock removed per day.

Table S4. Spearmann correlations between bacterivory measurements (protist ingestion rates and mixotrophs as proportions of heterotrophs and phototrophs) and environmental parameters and abundances.

Table S5. Recovered DGGE band sequences.

Please note: Wiley-Blackwell is not responsible for the content or functionality of any supporting materials supplied by the authors. Any queries (other than missing material) should be directed to the corresponding author for the article.